Improvement of ship hulls for comfort in passenger vessels

João Pedro Gil Rosa
joao.pedro.rosa@ist.utl.pt

Instituto Superior Técnico, Lisboa, Portugal

October 2019

Abstract

The objective of the work is to improve hulls from passenger vessels for comfort. The Overall Motion Sickness Index (OMSI), defined as the mean MSI value on the main deck, is used as the main parameter to be minimized, in order to obtain improved hulls for comfort. Two different passenger ships are submitted to various hull transformations in order to investigate their influence on passenger's comfort. These are categorized into two groups: geometric and hull from transformations. The transformations are performed using MaxSurf Modeler developed by Bentley systems, based on the Lackenby Method. Each new hull is submitted to a seakeeping analysis that accounts for various heading angles and a specific operating scenario, described by the JONSWAP Spectrum. An in-house strip theory code CENTEC-SK, developed at CENTEC in Instituto Superior Tcnico, is used to predict heave, roll and pitch motions at various headings. This program is selected based on a comparison between a commercially available software and experimental results from S-175 containership, collected by ITTC. The improved hulls, selected based on the study of OMSI, are compared to their parent hulls regarding their RAOs plots. A similar comparison is performed regarding the absolute vertical accelerations, at strategic locations on the main deck. In order to assess the influence of comfort-oriented hull transformations, on other parameters of the seakeeping performance of a ship, the hull resistance is compared between each hull transformation. Finally, the improved hull forms are compared to their parent hulls regarding their operability index based on comfort criteria.
Keywords: Passenger ship, Comfort, Motion sickness, Strip theory, Seakeeping analysis, Operability index

1. Introduction

For naval architects it is crucial to consider the performance of a ship, at an early design stage. One of its parameters is the seakeeping performance, which has been widely used since the development of practical strip theories. From which different tools can be used to check and optimize a certain ship's operability, regarding its motions as an example.

The seakeeping qualities depend not only on the expected seaway, but also on the ship's mission, that is, the type of service and topology. Particularly in passenger or cargo vessels the wellness and comfort on board, crew and passengers safety are the primary elements to be optimized. These qualities become even more important for passengers ships, when considering the collateral effect of seakeeping, the seasickness. These ship motions increase the amount of energy required form the crew. In addition it increases the level of fatigue and drowsiness on passengers, particularly in long journeys. It becomes a defining factor for certain passenger ships and ferries, where passengers can opt between different types of transportation. In terms of comfort, the seasickness produced by the ship's motion also effects the earnings obtained aboard the ship, since nauseate passengers are less likely to show interest on the extra services, such as shops, restaurants, etc. When it comes to safety, seasickness and motions also have harmful effects, particularly in emergency situations. In such conditions both crew and costumers have worsened performances.

Even though seakeeping qualities are not the only leading aspect on the design process, it is reasonable to work on possible improvements, despite certain fixed parameters. On passengers ships seakeeping optimization for habitability and operability has been continuously researched in past decades.

Kukner and Sariöz [11] studied the application of seakeeping analysis into early stages of ship design. A methodology for consistently generate new hull forms, based on Lackenby Method [12] was proposed. This work was further investigated by **Özüm et al.** [15]. **Cepowski** [5] studied the influence of variations in form coefficients, on the

seakeeping behaviour of a passenger-car ferry. **Scamardella and Piscopo** [18] used parametric modelling to generate several hull forms, that were used to compare the differences in passenger comfort level, on passenger ship, at various locations and sea-sates. Overall Motion Sicknes Index (OMSI) was introduced as the parameter to be minimized in this optimization procedures. More recently **Belga et al.** [2] optimized the hull form of a catamaran based on the Motion Sickness Index (MSI), to operate for an offshore platform at the Alentejo basin.

The objective of the present work is to optimize hulls from passenger ships for comfort. Overall Motion Sickness Index (OMSI) studied along the main deck was used as a parameter to be minimized in the optimization procedure. OMSI is an average value of Motion Sickness Index (MSI) that is based on absolute vertical accelerations. These are calculated for multiple locations along the deck, for different headings and sea-state. Two different passenger ships are considered (SHIP1 and SHIP2) accounting for both their operating scenario (Operating Scenario 1 and Operating Scenario 2) respectively. SHIP1 is design to operate on calm conditions, such as river and coastal waters. SHIP2 is to operate on ocean conditions. Various alternative hulls have been generated based on these parent ships. These derived hulls are obtained based on geometric and hull form transformations. The geometric transformations consist on the variation of the length at waterline L_{WL} and the breath at waterline B_{WL}. Hull form transformations are obtained using the Lackenby Method [12], where some hull form parameters such as the block coefficient (C_B), the midship section coefficient C_M) and the longitudinal center of buoyancy (LCB) position are varied. In order to compare the effect of each transformation on the seakeeping performance the Froude number of each parent ship is kept constant regarding the parent hull. Various headings are considered based on the probability distribution. The significant wave height and zero-crossing periods, based on a statistical analysis of the seaway are also considered in order to calculate OMSI. A hull resistance analysis is performed to all hull variations. The optimized hulls are finally compared to the parent hull regarding response amplitude operators (RAOs) peak, absolute vertical accelerations at relevant locations along the deck and on their operability index.

2. Background

2.1. Wave spectra theory

The formulation for the wave spectrum here presented is based on *MAXSURF* Motions user manual [3] and is a generalised spectrum formulation used by DNV, based on JONSWAP spectrum original developed by the Joint North Sea Wave Project. This spectrum has been widely used in the offshore industry and was seen as suitable to be used in the work. In the formulation presented $H_{1/3}$ corresponds to the wave height and T_P is the peak period. The spectrum is defined as follows:

$$S_\zeta(\omega_0) = \frac{\alpha}{\omega_0} e^{\frac{-\beta}{\omega_0}} \gamma^{e^{\frac{-1}{2\sigma^2}\left[\frac{\omega_0}{\omega_p}-1\right]^2}} \tag{1}$$

Where,

$$\alpha = 5\pi^4 (1 - 0.287 ln(\gamma)) \frac{H_{\frac{1}{3}}^2}{T_p^4} \tag{2}$$

$$\beta = \frac{20\pi^4}{T_p^4} \tag{3}$$

$$\gamma = \begin{cases} 5.0 & for \quad \frac{T_p}{\sqrt{H_{\frac{1}{3}}}} \leq 3.6 \\ e^{5.75 - \frac{1.15 T_p}{\sqrt{H_{\frac{1}{3}}}}} & for \quad 3.6 < \frac{T_p}{\sqrt{H_{\frac{1}{3}}}} \leq 5.0 \\ 1.0 & for \quad 5.0 < \frac{T_p}{\sqrt{H_{\frac{1}{3}}}} \end{cases} \tag{4}$$

$$\sigma = \begin{cases} 0.07 & for \quad \omega_0 < \omega_p \\ 0.09 & for \quad \omega_0 > \omega_p \end{cases}, \qquad \omega_p = \frac{2\pi}{T_p} \tag{5}$$

2.2. RMS Vertical Accelerations

The absolute vertical displacement (ξ_z) at a remote location (x', y' ,z') is given by Equation 6 assuming motions of generally small amplitude:

$$\xi_z(x', y', \omega) = \Re\left\{ \left[\xi_3^A(\omega) - x' \xi_5^A(\omega) + y' \xi_4^A(\omega) \right] e^{i\omega t} \right\} \tag{6}$$

Here ξ_j^A with j = 3,4,5 is the complex amplitude of the harmonic heave, roll and pitch motion, respectively. Let ω=ω_0, then the ship vertical responses on a given sea spectrum S_z is given by:

$$S_z(x', y', \omega_0) = |\xi_z(x', y', \omega_0)|^2 S_\zeta(\omega_0) \tag{7}$$

The spectral moment m_{2z} and m_{4z} are given by Equation 8 and 9 respectively. These formulation are proposed by Journe and Massie [10] as a means to avoid numerical errors for headings from quartering and following seas.

$$m_{2z} = \int_0^\infty \omega_e^2 \cdot S_z(\omega_e) \cdot d\omega_e = \int_0^\infty \omega_e^2 \cdot S_z(\omega_0) \cdot d\omega_0 \tag{8}$$

$$m_{4z} = \int_0^\infty \omega_e^4 \cdot S_z(\omega_e) \cdot d\omega_e = \int_0^\infty \omega_e^4 \cdot S_z(\omega_0) \cdot d\omega_0 \tag{9}$$

2.3. Motion Sickness Index (MSI)

Many proposals on how to predict motion sickness have been developed over the years, but Motion Sickness Index (MSI) is still one of the most famous and used today. The original model was originally developed by O'Hanlon and McCauley [14] and it assessed the number of passengers that vomit after two hours. This model was further developed by McCauley [13] to include a variable time domain. The formulation here presented to obtain MSI is based on this second iteration of the model and is

the same one used by *MAXSURF* Motions [4]. It was described by Colwell [6] and depends on the average RMS vertical acceleration $|RMS_{\mathrm{az}}|$, the average peak frequency of the vertical motions of the ship $|f_{\mathrm{e}}|$ and the voyage time (or period to which MSI is being tested) in minutes (t).

$$MSI\% = 100 \times \Phi(Z_a)\Phi(Z_t) \tag{10}$$

Where $\Phi(Z)$ is the standard normal distribution function:

$$\Phi(Z) = \frac{1}{\sqrt{2\pi}} e^{-\frac{z^2}{2}} \tag{11}$$

$$Z_a = 2.128 log_{10}(a) - 9.277 log_{10}(f_e) - 5.809\left[log_{10}(f_e)\right]^2 - 1.851 \tag{12}$$

$$Z_t = 1.134 Z_a + 1.989 log_{10}(t) - 2.904 \tag{13}$$

$$a = \frac{|RMS_{\mathrm{az}}|}{g} = \frac{0.798\sqrt{m_{4z}}}{g} \qquad |f_e| = \frac{\sqrt{\frac{m_{4z}}{m_{2z}}}}{2\pi} \tag{14}$$

2.4. Overall Motion Sickness Index (OMSI)

On classical seakeeping analysis the procedures to compare the parent hull with ship variation discard the operating scenarios and sea spectra. The classic rule of thumb is selecting the best hull as the one who minimizes heave and pitch RAOs. Head regular waves are usually considered, since they are considered to be the worst case scenario. However it is more reliable, to consider multiple sea-states that the ship may encounter during its life time compared to one single sea-sates. Also considering head seas as the worst case scenario is not always true, since MSI peaks may also occur at transverse headings depending on the wave peak period. Overall Motion Sickness Index (OMSI) developed by Scamardella and Piscopo [18] was considered as the ideal parameter to be minimized, on ship variations that seek to improve comfort on passenger ships. The optimized hulls are the solutions with smallest values of OMSI. Here MSI is considered on multiple locations along the deck, heading angles and sea states and averaged into a single factor, the OMSI. OMSI is defined as the mean MSI over the deck for any assigned sea-state and heading angle, as:

$$OMSI_{(H_{1/3},T_p)_j,\beta_k} = \frac{\int_{A_{deck}} MSI_{(H_{1/3},T_p)_j,\beta_k,(x',y',z'_{deck})} dA}{A_{deck}} \tag{15}$$

The notation (x', y', z'_{deck}) is used to denote the coordinates of the ith of $\mathrm{N_c}$ remote control location points on the main deck area ($\mathrm{A_{deck}}$) and β as the heading. OMSI is then defined for any assigned sea-state and heading angles:

$$OMSI_{(H_{1/3},T_p)_j,\beta_k} = \frac{1}{N_c} \sum_{i=1}^{Nc} MSI_{(H_{1/3},T_p)_j,\beta_k,(x',y',z'_{deck})_i} \tag{16}$$

Finally, accounting for all heading angles and peak periods:

$$OMSI = \frac{1}{N_c} \sum_{j=1}^{Ns} p_j \sum_{k=1}^{N_\beta} p_\beta \sum_{i=1}^{N_c} OMSI_{(H_{1/3},T_p)_j,\beta_k,(x',y',z'_{deck})_i} \tag{17}$$

Where $\mathrm{N_c}$, $\mathrm{N_s}$ and $\mathrm{N_\beta}$ denote the number of remote control location points on the main deck, sea states and heading angles, respectively. Both the sea-states and heading angles have a certain probability of occurrence $\mathrm{p_j}$ and $\mathrm{p_\beta}$, respectively.

3. Programs Validation

Strip theory was selected as the tool to perform the seakeeping analysis. It is to be embedded on hull optimization procedures, for passengers comfort, of two different types of passenger ships. Programs using the strip theory, must be time efficient while maintaining good level of accuracy. Motivating the comparison of two available code alternatives, **CENTEC-SK** and ***MAXSURF* Motions**, at different headings and for a fixed Froude number. Belga [1] made a similar comparison on the same programs but only for head waves and multiple Froude numbers instead. Both codes perform the computations in the frequency domain, following the common method of Salvesen et al. [17].

3.1. Overview of seakeeping program, *CENTEC-SK*

CENTEC-SK was developed at CENTEC (Center for Marine Technology and Ocean Engineering) at Instituto Superior Técnico (IST), Lisbon. It is a frequency domain strip-theory code or the linear version of Fonseca and Guedes Soares [7]. The available documentation was used, however many of its features were not documented. It is known that it follows the frequency domain formulation of Salvesen et al. [17] without transom terms in the equations. According to Belga [1] the numerical solution for the 2-D radiation potential in forced harmonic motions, which allows to determine the sectional added masses, damping coefficients and diffraction force is obtained, via multi-parameter conformal mapping Ramos and Guedes Soares [16]. The linear potential flow theory requires the correction for viscous damping for the case of roll motions.

3.2. Overview of seakeeping program *MAXSURF* Motions

MAXSURF Motions is one module within *MAXSURF* Connected Edition V21 which is a commercially available software developed by Bentley Systems [4]. This software is very well documented. The configuration set for comparison uses the linear strip theory of Salvesen et al. [17] and without transom corrections. The numerical solution for 2-D radiation potential is also obtained via multi-parameter conformal mapping. The roll response is

calculated using linear roll damping theory. This program is very user friendly and the modules are easy to integrate between each other, making it simple to perform changes on the input file. However the running time can be very long and it is difficult to perform multiple tests.

3.3. Program Validation

The comparison process is simplified for the present study. It is done by analyzing the accuracy of the RAOs, from the programs with experimental results available in the literature. Since neither one of the two ships at study have available experimental results, it was selected an alternative ship for the comparison with similar characteristics and very well know to the industry, the S-175 containership.

The validation is performed by comparing the measure data and the calculations for the responses in regular waves for the S-175 containership with a forward speed corresponding to a Froud number of Fn=0.275. This comparison focuses on the transfer functions for heave, roll and pitch at six different heading angles (β=180°, β=150°, β=120°,β=90°, β=60° and β=30°). β=180° is head seas, β=90° is beam seas and β=0° is following seas, following International Towing Tank Conference ITTC standard definitions. The results are plotted against the non-dimensional wave frequency $\omega\sqrt{L/g}$ with a 31 evenly spaced frequencies in regular waves. The responses have been measured at a wave height of 1/50 of Lpp. The non-dimensional parameters, such as heave per wave amplitude, pitch and roll per wave slope are presented in the results. The validation for the above modes of motion for the S-175 container ship in regular waves, based on the transfer function of the motion, is carried out by comparing the computational results from the numerical code with experimental date available in the literature. The experimental data used in the validation process is from three organizations Ishikawajima-Harima Heavy Industries (IHI), Sumitomo Heavy Industry (SHI) and Ship Research Institute (SRI), presented in the summery report of the seakeeping committee of the 15$^{\text{th}}$ and 16$^{\text{th}}$ International Towing Tank Conferences, ITTC [9]. Three different institutions were selected because there were no consistent experimental results for all headings of interest thus becoming the best solution to validate both programs. In this extended summary only some meaningful results were selected and are presented on Figures 1 - 3. It should be noticed that the experimental data was not enough on the measured roll transfer function, specially, at the resonance frequency. For that reason such results can not be confirmed with the same accuracy as heave and pitch.

For the S-175 containership, the comparisons show that both programs predict consistent results regarding heave and pitch motions. Particularly in heave motions, no noticeable differences were found between the two programs at any of the 6 headings studied. On pitch motions *MAXSURF* Motions over predicted the results, for headings between the beam and following seas. Regarding roll motions, the results were not confirmed by the experimental results, since the frequency region for the resonance peak, the one of most interest, was not within the region of the experimental results. However it is clear that *MAXSURF* Motions over predicts the resonance peak of roll motions compared to *CENTEC-SK*. It is easier to include roll damping corrections on the later one, showing clear effect on the results. Thus concluding that *CENTEC-SK* code is the most suitable tool for this dissertation and *CENTEC-SK* is used to obtain all seakeeping results. Its fast computation and flexibility to integrate with with *MATLAB*, makes it the best tool for multiple and reliable seakeeping calculations. Its drawbacks are the lack of official documentation and laborious input files.

4. Characterization of the seakeeping optimization process

4.1. Parent ships characteristics

Two different ships were selected to be optimized. The first ship is characteristics of river and coastal waters and is here refereed as **SHIP1**. This ship hull has simple lines that make it easy to manipulate as shown on Figure 4. Its main dimensions are presented on Table 1. The passengers comfort was analysed along the length of its deck, meaning that a large area with points is considered when calculating OMSI, as shown on Figure 5. The second ship is to operate on ocean going routs and is here refereed as **SHIP2**. Its lines are also simple and easy to manipulate as shown on Figure 6. Its main dimensions are presented on Table 2. Unlike on SHIP1, in this second ship a specific area with points is now considered when calculating the OMSI, as shown on Figure 7.

Table 1: Parent hull main dimensions and form parameters [SHIP1].

Displacement	$\triangle$	960.5	[t]
Draft to baseline	T	1.6	[m]
Waterline length	L_{WL}	75	[m]
Waterline beam	B_{WL}	11	[m]
Prismatic coefficient	C_P	0.717	[-]
Block Coefficient	C_B	0.71	[-]
Midship section coefficient	C_M	0.99	[-]
Waterplane area coefficient	C_{WP}	0.841	[-]
LCB=LCG from MS (-ve aft)	LCB =LCG	-1.5	[m]
Vertical center of buoyancy	KB	0.859	[m]
Vertical center of gravity	KG	3.58	[m]
Speed (Maximum)	V	16	[kn]

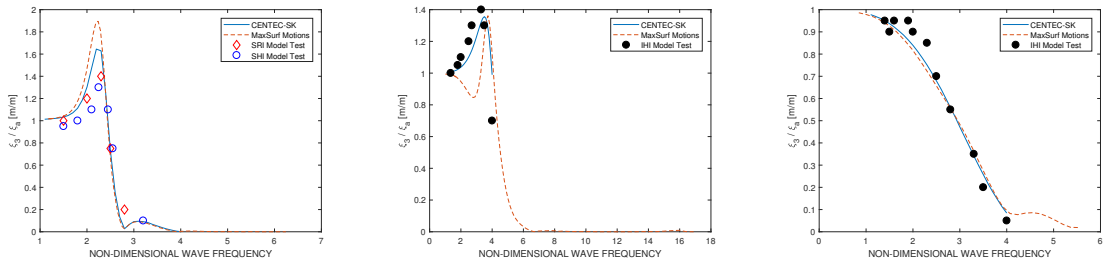

(a) β=180° (b) β=90° (c) β=60°

Figure 1: Heave RAOs as function of the wave frequency

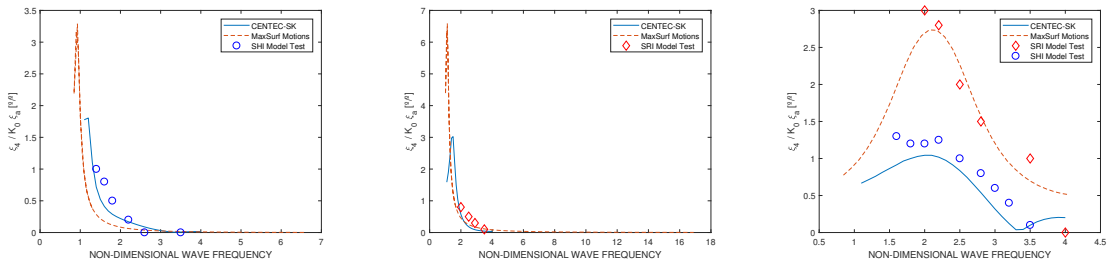

(a) β=150° (b) β=90° (c) β=30°

Figure 2: Roll RAOs as function of the wave frequency

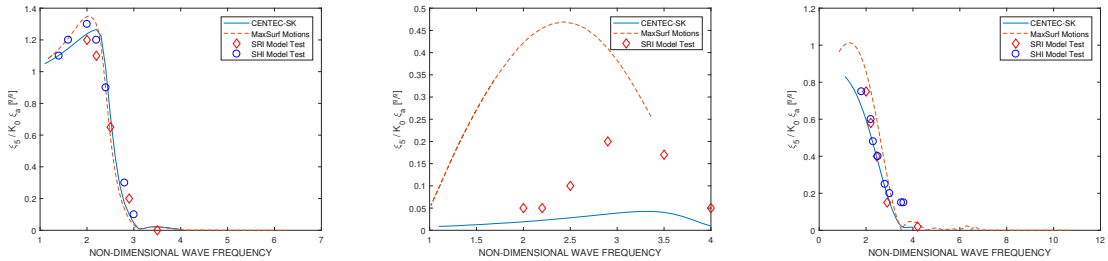

(a) β=180° (b) β=90° (c) β=30°

Figure 3: Pitch RAOs as function of the wave frequency

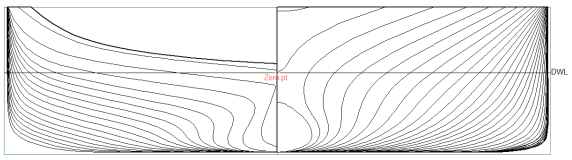

Figure 4: Parent hull forms from *MAXSURF* Modeler [SHIP1].

Figure 5: Distribution of points along the deck [SHIP1]

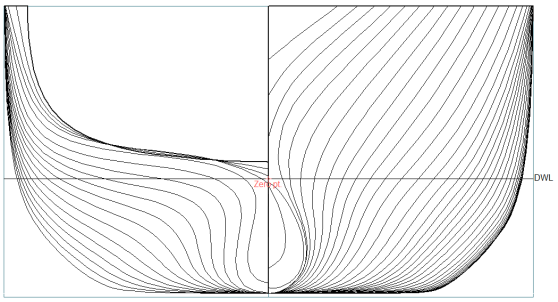

Figure 6: Parent hull forms from *MAXSURF* Modeler [SHIP2].

4.1.1 Operating sites

4.2. Coast of Algarve [Operating Scenario 1]

SHIP1 operates on the basin of Algarve, for touristic trips along the coast, called **Operating Scenario 1**. The characterization of the sea is done using a scatter diagram presented on Table 3. It was constructed based on data collected by CENTEC (Center for Marine Technology and Ocean En-

Table 2: Parent hull main dimensions and form parameters [SHIP2].

Displacement	$\triangle$	5085	[t]
Draft to baseline	T	4.5	[m]
Waterline length	L_{WL}	98	[m]
Waterline beam	B_{WL}	20	[m]
Prismatic coefficient	C_P	0.642	[-]
Block Coefficient	C_B	0.563	[-]
Midship section coefficient	C_M	0.877	[-]
Waterplane area coefficient	C_{WP}	0.719	[-]
LCB=LCG from MS (-ve aft)	LCB =LCG	-2.9	[m]
Vertical center of buoyancy	KB	2.5	[m]
Vertical center of gravity	KG	6.5	[m]
Speed (Service)	V	21	[kn]

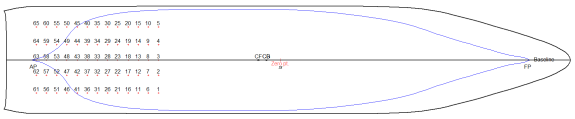

Figure 7: Distribution of points along the deck [SHIP2]

gineering) at Instituto Superior Tcnico (IST). This data was gathered in one point near the coast of Algarve [Φ37N, L -8.5W], for a period between 1958 and 2001. There are 10 different intervals of wave height ($H_{1/3}$) to 22 different peak periods (T_P). The wave spectrum for each sea state $S_\zeta(\omega_0)$ is calculated based on these data.

Statistical information of sea direction is also available and considering a trip from West to East the ship faces the worst scenario of encountering waves. Figure 8 presents the probability distribution of the ship-wave headings for SHIP1. It is mainly constituted by head and bow seas. It means that for this type of operation: beam, quartering and following seas will have little influence on the OMSI. The best results should be on hull variations that mainly improve comfort on head seas, which correspond to around 62% on encountered seas.

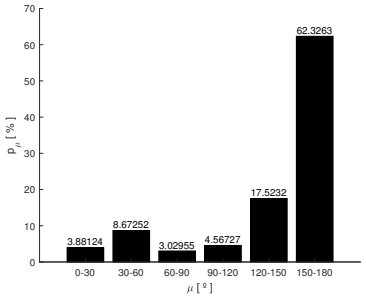

Figure 8: Probable fractions of time at various ship-wave headings [SHIP1]

4.3. Atlantic Ocean region between Algarve and Madeira [Operating Scenario 2]

SHIP2 operates on the Atlantic Ocean connecting Algarve to Madeira, transporting passengers between the two regions. This operating scenario is called **Operating Scenario 2**. The characterization of the sea is done using a scatter diagram presented in Table 4. It is constructed based on data collected by the European Centre for Medium-Range Weather Forecasts (ECMWF). This data is representative of one point in the middle of the route [Φ35 N, L 15 W], for a period between 1979 and 2013. There are 10 different intervals of wave height ($H_{1/3}$) to 20 different peak periods (T_P). The wave spectrum for each sea state $S_\zeta(\omega_0)$ is calculated for these sea-states. Statistical information of sea direction is also available and a trip from Northeast to Southwest is considered. For this trip it is expected to encounter mainly head and bow seas and sometimes beam seas as show in Figure 9.

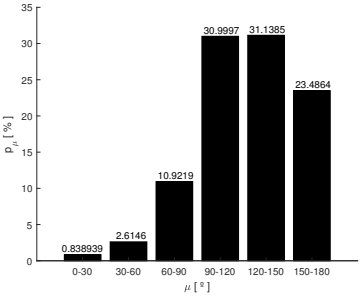

Figure 9: Probable fractions of time at various ship-wave headings [SHIP2]

4.4. Derivation of new hull forms

Several hull variations were obtained from both parent hulls. Such variations were divided into two categories. The first category is focused on the systematical variation of form parameters such as the longitudinal center of buoyancy (LCB), the block coefficient (C_B) and the midship section coefficient (C_M), using the Lackenby Method [12]. The second type of systematical variations only depended on main dimensions, such as the length at waterline (L_{WL}), beam at waterline (B_{WL}) and draft (T). This methodology for developing new hull forms is based on the work of Grigoropoulos and Loukakis [8], Kukner and Sariöz [11], Özüm et al.[15], Cepowski [5], Scamardella and Piscopo [18] and Belga et al [2], who proved that seakeeping performances are affected by these parameters.

Six different types of hull variations were tested in this dissertation. All six on SHIP1 and four on SHIP2. Each hull variation was performed using *MAXSURF* Modeler from *Bentley Systems* [3], where all the transformations were easily accomplished for a large number of hulls. In order to make the discussion as clear as possible, each type of hull transformations was called **Set n**. With n being a number between 1-6 that corresponds to each method of transformation. Set 1-3 corresponds to transformations of block coefficient (C_B) and longitudinal center of buoyancy (LCB) differing on which parameters were

Table 3: Joint frequency of significant wave height and spectral peak period. Representative data for the coast of Algarve.

Significant wave height [m]	Spectral peak period (s)																			
	3	**4**	**5**	**6**	**7**	**8**	**9**	**10**	**11**	**12**	**13**	**14**	**15**	**16**	**17**	**18**	**19**	**20**	**21**	**22**	**Sum**
1	508	9992	18888	6858	2900	2871	4174	4963	5661	5847	4854	3171	1651	0	676	356	0	65	0	13	73448
2	0	101	5072	8450	6026	1332	1609	1913	2443	2838	3692	3582	2688	0	1419	899	0	111	0	34	42209
3	0	0	2	251	1971	1251	828	735	649	552	727	661	562	0	377	374	0	32	0	6	8978
4	0	0	0	2	38	223	500	427	378	199	212	197	217	0	83	134	0	2	0	0	2612
5	0	0	0	0	0	5	42	142	215	182	83	50	56	0	59	55	0	1	0	0	890
6	0	0	0	0	0	0	0	11	60	99	35	26	21	0	27	15	0	1	0	0	295
7	0	0	0	0	0	0	0	0	6	25	24	14	14	0	8	15	0	0	0	0	106
8	0	0	0	0	0	0	0	0	1	2	2	2	1	0	2	12	0	0	0	0	22
9	0	0	0	0	0	0	0	0	0	1	1	1	0	0	0	1	0	0	0	0	4
10	0	0	0	0	0	0	0	0	0	0	1	2	0	0	0	0	0	0	0	0	3
Sum	508	10093	23962	15561	10935	5682	7153	8191	9413	9745	9631	7706	5210	0	2651	1861	0	212	0	53	128567

Table 4: Joint frequency of significant wave height and spectral peak period. Representative data for the Atlantic Ocean (Region between Algarve and Madeira)

Significant wave height [m]	Spectral peak period (s)															
	5	**6**	**7**	**8**	**9**	**10**	**11**	**12**	**13**	**14**	**15**	**16**	**17**	**18**	**19**	**20**	**Sum**
1	6	38	244	238	241	128	58	42	17	26	4	0	4	0	0	0	1046
2	7	360	2235	2160	3094	3318	3638	4125	2870	1007	239	8	26	3	0	0	23090
3	0	11	570	1183	1583	1237	1290	2380	4150	4008	1505	59	258	38	0	2	18274
4	0	0	0	77	278	426	477	526	809	1502	1529	89	447	69	0	2	6231
5	0	0	0	2	8	64	130	216	218	298	404	36	358	71	0	2	1807
6	0	0	0	0	1	3	15	54	73	69	115	12	108	39	1	5	495
7	0	0	0	0	0	0	0	4	14	20	37	5	52	15	0	0	147
8	0	0	0	0	0	0	0	0	1	5	21	1	6	3	0	0	37
9	0	0	0	0	0	0	0	0	0	1	3	0	1	3	0	0	8
10	0	0	0	0	0	0	0	0	0	0	1	0	0	0	0	0	1
Sum	13	409	3049	3660	5205	5176	5608	7347	8152	6936	3858	210	1260	241	1	11	51136

free to change when the parent hull was being manipulated on *MAXSURF* Modeler. On **Set 1** only the displacement was free to change. On **Set 2** only draft was free to to change. On **Set 3** both beam and draft were free to change while maintaining the same B/T ratio. The goal on this three sets was to see if there would be any clear differences on OMSI if the coefficients were obtained by the manipulation of different variables. **Set 4** corresponds to hull transformations based on the midship section coefficient (C_M). **Set 5** corresponds to geometrical hull transformations based on the length at waterline (L_{WL}). **Set 6** corresponds to geometrical hull transformations based on the beam at waterline (B_{WL}). In the following tables the data refereeing to each hull variation is presented. Tables 5-10 are referent to SHIP1. Tables 11-14 are referent to SHIP2. On these tables is clear how each coefficient is varied and which parameters were fixed for each **Set n**, where the data in bold is refer to the parent hull/ship.

Table 5: Hull form parameters for Set 1 of variations. Fixed C_M = 0.99, L_{WL} = 75 m, B_{WL} = 11 m and T = 1.6 m. Parent ship: SHIP1.

	C_B = 0.66	C_B= 0.68	C_B = 0.70	C_B = 0.71	C_B= 072	C_B = 0.74	C_B = 0.76
LCB = 50%							
C_P	0.67	0.69	0.707		0.727	0.748	0.780
C_{WP}	0.817	0.828	0.843	-	0.857	0.871	0.885
Δ	901 t	920 t	948 t		974 t	1001 t	1028 t
LCB = 52%							
C_P	0.67	0.69	0.707	**0.717**	0.727	0.748	0.78
C_{WP}	0.809	0.818	0.833	**0.841**	0.848	0.862	0.876
Δ	901 t	920 t	948 t	**960.5 t**	974 t	1001 t	1028 t
LCB = 54%							
C_P	0.67	0.69	0.707		0.727	0.748	0.78
C_{WP}	0.801	0.809	0.824	-	0.838	0.853	0.867
Δ	901 t	920 t	948 t		974 t	1001 t	1028 t

Table 6: Hull form parameters for Set 2 of variations. Fixed C_M = 0.99, L_{WL} = 75 m, B_{WL} = 11 m and Δ= 960.5 t. Parent ship: SHIP1

	C_B = 0.66	C_B= 0.68	C_B = 0.70	C_B = 0.71	C_B= 072	C_B = 0.74	C_B = 0.76
LCB = 50%							
C_P	0.667	0.687	0.707		0.727	0.748	0.768
C_{WP}	0.809	0.825	0.84	-	0.855	0.869	0.883
T	1.721 m	1.671 m	1.623 m		1.578 m	1.535 m	1.495 m
LCB = 52%							
C_P	0.667	0.687	0.707	**0.717**	0.727	0.748	0.768
C_{WP}	0.803	0.818	0.833	**0.841**	0.848	0.862	0.876
T	1.721 m	1.671 m	1.623 m	**1.6 m**	1.578 m	1.535 m	1.495 m
LCB = 54%							
C_P	0.667	0.687	0.707		0.727	0.748	0.768
C_{WP}	0.794	0.810	0.825	-	0.839	0.853	0.867
T	1.721 m	1.671 m	1.623 m		1.578 m	1.535 m	1.495 m

5. Results

5.1. Results from OMSI analysis

The Overall Motion Sickness Index (OMSI) is analysed for all types of hull variation, at their re-

Table 7: Hull form parameters for Set 3 of variations. Fixed $C_M = 0.99$, $L_{WL} = 75$ m, $B_{WL}/T = 6.9$ and $\Delta = 960.5$ t. Parent ship: SHIP1.

	$C_B = 0.66$	$C_B = 0.68$	$C_B = 0.70$	$C_B = 0.71$	$C_B = 072$	$C_B = 0.74$	$C_B = 0.76$
LCB = 50%							
C_P	0.666	0.687	0.707		0.728	0.748	0.768
C_{WP}	0.813	0.828	0.843	-	0.857	0.871	0.885
T	1.659 m	1.635 m	1.611 m		1.589 m	1.567 m	1.546 m
B_{WL}	11.41 m	11.24 m	11.078 m		10.923 m	10.775 m	10.632 m
LCB = 52%							
C_P	0.666	0.687	0.707	**0.717**	0.728	0.748	0.768
C_{WP}	0.803	0.818	0.833	**0.841**	0.848	0.862	0.876
T	1.659 m	1.635 m	1.611 m	**1.6 m**	1.589 m	1.567 m	1.546 m
B_{WL}	11.41 m	11.24 m	11.078 m	**11 m**	10.923 m	10.775 m	10.632 m
LCB = 54%							
C_P	0.666	0.687	0.707		0.728	0.748	0.768
C_{WP}	0.794	0.809	0.824	-	0.838	0.853	0.867
T	1.659 m	1.635 m	1.611 m		1.589 m	1.567 m	1.546 m
B_{WL}	11.41 m	11.24 m	11.078 m		10.923 m	10.775 m	10.632 m

Table 8: Hull form parameters for Set 4 of variations. Fixed $C_B = 0.71$, $B_{WL} = 11$ m, T = 1.6 m and $\Delta = 960.5$ t.Parent ship: SHIP1.

	$C_M = 0.99$	$C_M = 0.98$	$C_M = 0.97$	$C_M = 0.96$	$C_M = 0.95$
LCB = 52%					
C_P	**0.717**	0.725	0.733	0.742	0.75
C_{WP}	**0.841**	0.845	0.847	0.852	0.855

Table 9: Hull form parameters for Set 5 of variations. Fixed $C_B = 0.71$, $C_P = 0.717$, $C_M = 0.99$, $B_{WL}/T = 6.87$ and $\Delta = 960.5$ t. Parent ship: SHIP1.

	$L_{WL} = 90\%$	$L_{WL} = 95\%$	$L_{WL} = 100\%$	$L_{WL} = 105\%$	$L_{WL} = 110\%$
LCB = 52%					
L_{WL}	67.5 m	71.25 m	**75 m**	78.75 m	82.5 m
B_{WL}	11.60 m	11.30 m	**11 m**	10.74 m	10.50 m
T	1.69 m	1.64 m	**1.6 m**	1.561 m	1.53 m

Table 10: Hull form parameters for Set 6 of variations. Fixed $C_B = 0.71$, $C_P = 0.717$, $C_M = 0.99$, $L_{WL} = 75$ m and $\Delta = 960.5$ t. Parent ship: SHIP1

	$B_{WL}/T = 5.2$	$B_{WL}/T = 5.8$	$B_{WL}/T = 6.87$	$B_{WL}/T = 7.9$	$B_{WL}/T = 8.6$
LCB = 52%					
B_{WL}	9.5 m	10.15 m	**11 m**	11.8 m	12.3 m
T	1.852 m	1.734 m	**1.6 m**	1.491 m	1.431 m

Table 11: Hull form parameters for Set 2 of variations. Fixed $C_M = 0.877$, $B_{WL} = 20$ m and $\Delta = 5085$ t. Parent ship:SHIP2.

	$C_B = 0.50$	$C_B = 0.53$	$C_B = 0.56$	$C_B = 0.58$	$C_B = 0.60$
LCB = 50%					
C_P	0.57	0.604		0.661	0.684
C_{WP}	0.652	0.688	-	0.745	0.768
T	5.07 m	4.78 m		4.37 m	4.23 m
LCB = 53%					
C_P	0.57	0.604	**0.642**	0.661	0.684
C_{WP}	0.644	0.680	**0.719**	0.738	0.76
T	5.07 m	4.78 m	**4.5 m**	4.37 m	4.23 m
LCB = 56%					
C_P	0.57	0.604		0.661	0.684
C_{WP}	0.636	0.672	-	0.730	0.752
T	5.07 m	4.78 m		4.37 m	4.23 m

Table 12: Hull form parameters for Set 4 of variations. Fixed $C_B = 0.563$, $B_{WL} = 20$ m, T = 4.5 m and $\Delta = 5085$ t. Parent ship: SHIP2.

	$C_M = 0.79$	$C_M = 0.83$	$C_M = 0.87$	$C_M = 0.92$	$C_M = 0.96$
LCB = 53%					
C_P	0.714	0.679	**0.642**	0.612	0.587
C_{WP}	0.758	0.738	**0.719**	0.71	0.702

spective sea environment and for six different headings. The maximum service speed is considered, which for SHIP1 is 16kn and for SHIP2 is 21kn. These following results are obtained from a program developed in MATLAB MathWorks.

Table 13: Hull form parameters for Set 5 of variations. Fixed $C_B = 0.563$, $C_P = 0.642$, $C_M = 0.877$, $B_{WL}/T = 4.4$ and $\Delta = 5085$ t. Parent ship: SHIP2.

	$L_{WL} = 90\%$	$L_{WL} = 95\%$	$L_{WL} = 100\%$	$L_{WL} = 105\%$	$L_{WL} = 110\%$
LCB = 53%					
L_{WL}	93 m	96 m	**98 m**	100 m	19.50 m
B_{WL}	20.52 m	20.20 m	**20 m**	19.69 m	4.39 m
T	4.62 m	4.54 m	**4.5 m**	3.362 m	3.310 m

Table 14: Hull form parameters for Set 6 of variations. Fixed $C_B = 0.563$, $C_P = 0.642$, $C_M = 0.877$, $L_{WL} = 98$ m and $\Delta = 5085$ t. Parent ship: SHIP2.

	$B_{WL}/T = 3.33$	$B_{WL}/T = 3.77$	$B_{WL}/T = 4.44$	$B_{WL}/T = 5.10$	$B_{WL}/T = 5.55$
LCB = 53%					
B_{WL}	17.4 m	18.5 m	**20 m**	21.5 m	22.35 m
T	5.17 m	4.87 m	**4.5 m**	4.20 m	4.03 m

5.1.1 OMSI results for hull variation based on SHIP1

Hull variations derived from changing the C_B and shifting the LCB position indicate that OMSI is reduced by both increasing C_B and moving LCB forward, as seen in Tables 15, 16 and 17. For SHIP1 the effect off shifting LCB is not as clear as of changing C_B. This can be explain by the type of points distribution along the deck, see Figure 5. Since the points are equally distributed along the ship deck any improvements on one extremity of the ship will degrade the other and vice versa. Nevertheless the method still gives an optimized solution, based on the configurations that have smaller MSI values overall. In this dissertation an optimized solution is considered when OMSI is reduced. It is also important to notice that the improvements on OMSI are consistent in all three tables. That is, regardless of the method used to change C_B and LCB. Either using Set 1, Set 2 or Set 3, the OMSI was smaller on the highest C_B and lowest LCB. In all three cases the increase of C_B at a constant C_M will always benefit OMSI.

The variations performed using a $C_B = 0.76$ together with a shift of LCB to the midship gives the most comfortable hull. When C_B is transformed using the Set 1 for hull variations (variable displacement), the reduction of OMSI was in the order of 12.9% compared to the parent hull. Using Set 2 for hull variation (variable T do change the C_B), the reduction on OMSI was in the order of 17.7% compared to the parent hull. On the Set 3 of hull variations (variable T and B_{WL}) the reduction on OMSI was in the order of 12.4%. The results variations presented in Table 16 seem to consistently give slightly smaller results of OMSI. Such differences are explained by the fact that the B_{WL}/T is different for each new C_B, and an increase in this ratio is beneficial for the OMSI. Nevertheless, the goal of using three different sets to change C_B and LCB was achieved. The results were consistent on all three sets, showing that the results are not af-

fect by how each coefficient was obtained. Still, it was possible to select a solution that least affect the original design of the hull. For SHIP1 it is best to only change the draft of the ship, instead of changing the displacement (Set 1) or even the beam and draft simultaneously (Set 3).

Table 15: Values of OMSI on each hull variation based on Set 1 [SHIP1].

	CB = 0.66	CB = 0.68	CB = 0.70	CB = 0.71	CB = 0.72	CB=0.74	CB=0.76
LCB = 50%	4.637	4.487	4.280	-	4.089	3.942	3.787
LCB = 52%	4.761	4.630	4.438	**4.349**	4.228	4.048	3.854
LCB = 54%	4.869	4.758	4.511	-	4.032	4.078	3.863

Table 16: Values of OMSI on each hull variation based on Set 2 [SHIP1].

	CB = 0.66	CB = 0.68	CB = 0.70	CB = 0.71	CB = 0.72	CB=0.74	CB=0.76
LCB = 50%	4.727	4.538	4.383	-	4.102	3.862	3.581
LCB = 52%	4.855	4.612	4.489	**4.349**	4.386	4.018	3.652
LCB = 54%	4.985	4.662	4.535	-	4.281	3.987	3.725

Table 17: Values of OMSI on each hull variation based on Set 3 [SHIP1].

	CB = 0.66	CB = 0.68	CB = 0.70	CB = 0.71	CB = 0.72	CB=0.74	CB=0.76
LCB = 50%	4.728	4.055	4.261	-	4.101	3.975	3.808
LCB = 52%	4.870	4.294	4.483	**4.349**	4.254	4.051	3.863
LCB = 54%	4.818	4.367	4.572	-	4.365	4.158	3.900

The form variation obtained by reducing C_M (Set 4) is beneficial to OMSI. As shown in Table 18, such reductions consistently give smaller values of OMSI. The smallest of all is for a $C_M = 0.95$, where OMSI is reduced by 7.2% compared to the parent hull. This reductions may not seem as significant, but it is worth noticing that a $C_M = 0.95$ is less than 5% difference compared to $C_M = 0.99$. This is an interesting result, because not only the seakeeping is improved, while no major changes in the hull were introduced to do so.

Table 18: Values of OMSI on each hull variation based on Set 4 [SHIP1].

	CM = 0.99	CM = 0.98	CM = 0.97	CM = 0.96	CM = 0.95
LCB = 52%	**4.349**	4.213	4.147	4.157	4.038

The first geometrical variation in study or Set 5 of hull variations, was the variation of L_{WL}. Looking at Table 19 the increase in L_{WL} clearly reduces OMSI. Particularly an increase by 10% reduced OMSI by 28.5% compared to the parent hull. Making it the lowest OMSI from all the transformations performed to SHIP1.

Finally, the results for the second type geometrical variation or Set 6 of hull variations, were also obtained. Increasing the B_{WL}/T ratio reduces OMSI, as shown in Table 20. The change in ratio already seemed to give the advantage to the transformations of C_B by only changing T, as shown in Table 16. The increase in ratio by 25% reduced OMSI by 8.2%, which is not as significant as changes in L_{WL}.

Table 19: Values of OMSI on each hull variation based on Set 5 [SHIP1].

	L_{WL}= 90 %	L_{WL} = 95%	L_{WL} = 100%	L_{WL} = 105%	L_{WL} = 110%
LCB = 52%	5.378	4.836	**4.349**	3.808	3.109

Table 20: Values of OMSI on each hull variation based on Set 6 [SHIP1].

	B_{WL}/T = 75%	B_{WL}/T = 85%	B_{WL}/T = 100%	B_{WL}/T = 115%	B_{WL}/T = 125%
LCB = 52%	4.553	4.440	**4.349**	4.042	3.992

5.1.2 OMSI results for hull variation based on SHIP2

The OMSI on various hull variations was also studied on SHIP2. This is a different ship but still with the same type of hull transformations, namely: Set 2, Set 4, Set 5 and Set 6. By using another ship with the same type of transformations the performance of OMSI from different ships, sea-state conditions and studied locations can be studied. The first thing to be noticed is that OMSI on SHIP2 is much higher than before. Now the parent hull [SHIP2] has an OMSI = 16.106. This value is considerably higher than an OMSI = 4.349 from SHIP1. It can be explained by the harsher sea conditions and by the smaller area on the aft region, where points are distributed.

For SHIP2 only Set 2 was used to perform hull variations of C_B and LCB. According to Table 21, increasing C_B still contributes to reduce OMSI. In fact OMSI reduced by 17.6% when comparing the parent hull with the hull variation with the lowest OMSI, as expected from the previous results. On the other hand the best hull variation is now the one where LCB = 56%, which is the one further away from the midship. An interesting but predictable result, that shows how reducing the distance between the area where comfort is to be improved and the center of buoyancy is clearly valid. However it should be clear that the opposite is also true and some areas of the ship will degrade by such actions.

Table 21: Values of OMSI on each hull variation based on Set 2 [SHIP2].

	CB = 0.50	CB = 0.53	CB = 0.56	CB=0.58	CB=0.60
LCB = 50%	18.137	17.987	-	16.915	15.552
LCB = 53%	16.588	16.332	**16.106**	15.025	15.098
LCB = 56%	15.938	15.739	-	14.678	13.267

Reductions of C_M once again proved to be effective on reducing OMSI, as shown in Table 22. With a reduction of 14.5% from the parent hull. Yet the increase of C_M also improved the OMSI, which is

not to be expected. A possible reason for this unexpected results may be due to a distortion on the hull transformations, particularly on the bulb region. This distortion improved OMSI in the order of 9.4%. Its validity however can not be confirmed, since the distortions on the bulb may too be influencing it.

Table 22: Values of OMSI on each hull variation based on Set 4 [SHIP2].

	CM = 0.79	CM = 0.83	CM = 0.87	CM = 0.92	CM = 0.96
LCB = 53%	13.775	15.654	**16.106**	14.756	14.591

More in line with previous results are the geometrical hull variations. As shown in Table 23 the increase in L_{WL} reduced once again the OMSI. The reduction is in the order of 9.2% compared to the parent hull. The increase in ratio B_{WL}/T also proved beneficial to the OMSI, as shown on Table 24. This reduction was of 10.4% compared to the parent hull.

The difference between the two types of geometrical variations is in this case very similar unlike it was on SHIP1. It means that each variation does not influence every hull types exactly the same way, depending on the type of ship, the operating scenario and the significant type of headings. An optimization is then affected by both the type of hull, the method in use, together with sea environments and deck locations being improved.

Table 23: Values of OMSI on each hull variation based on Set 5 [SHIP2].

	L_{WL}= 90 %	L_{WL} = 95%	L_{WL} = 100%	L_{WL} = 105%	L_{WL} = 110%
LCB = 53%	16.553	16.569	**16.106**	14.892	14.625

Table 24: Values of OMSI on each hull variation based on Set 6 [SHIP2].

	B_{WL}/T = 75%	B_{WL}/T = 85%	B_{WL}/T = 100%	B_{WL}/T = 115%	B_{WL}/T = 125%
LCB = 53%	18.122	16.802	**16.106**	14.369	14.435

5.2. Comparison between heave, roll and pitch motions

The optimized results from the OMSI analysis for each ship at each Set n where compared to the parent ship, regarding the heave, pitch and roll RAOs. Each type of RAO was plotted at four different headings (180°, 120°, 90° and 60°). In this extended summary only the plots comparing the optimized hull obtained from Set 2, C_B = 0.76 and LCB = 50%, 52% and 54% with the parent hull C_B = 0.71 and LCB = 52% are presented, due to lack of space. These can be found on Figures 10 - 12.

The RAOs comparison proved that the reductions on OMSI were directly linked to reductions on ship motions for both SHIP1 and SHIP2.

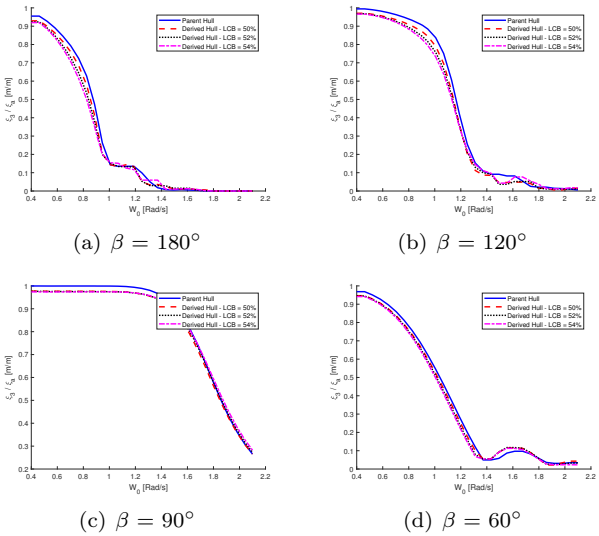

(a) $\beta = 180°$ (b) $\beta = 120°$

(c) $\beta = 90°$ (d) $\beta = 60°$

Figure 10: Heave RAOs. Parent Ship: SHIP1 with C_B = 0.71. Derived Hulls: Set 2 with C_B = 0.76.

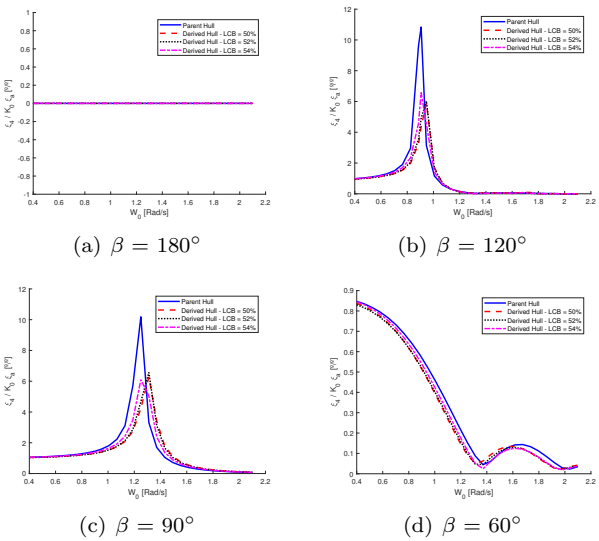

(a) $\beta = 180°$ (b) $\beta = 120°$

(c) $\beta = 90°$ (d) $\beta = 60°$

Figure 11: Roll RAOs. Parent Ship: SHIP1 with C_B = 0.71. Derived Hulls: Set 2 with C_B = 0.76.

5.3. Absolute vertical accelerations

Absolute vertical accelerations responses as function of encounter frequency are compared in this section. Since so many sea-states, headings and deck locations were used it would be impractical to compare every single one of them. For that reason a sea-state with $H_{1/3}$ = 1 m and T_P = 9 s is selected for comparison and the same headings used to compare RAOs are used to compare absolute vertical accelerations. Different points were selected to be studied on both ships and their locations are found on Table 25 and Table 26. Figures 13-14 correspond to such comparison between the parent hull SHIP1 and the optimized hull C_B =

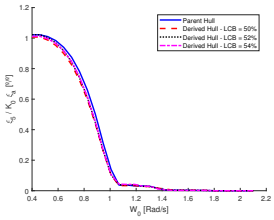

(a) $\beta = 180°$

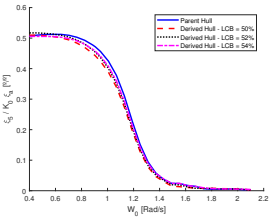

(b) $\beta = 120°$

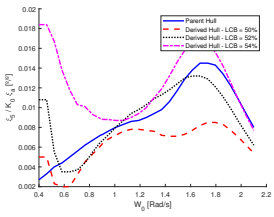

(c) $\beta = 90°$

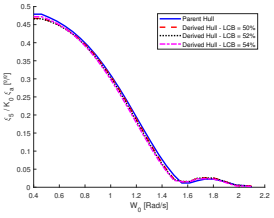

(d) $\beta = 60°$

Figure 12: Pitch RAOs. Parent Ship: SHIP1 with $C_B = 0.71$. Derived Hulls: Set 2 with $C_B = 0.76$.

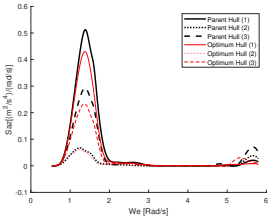

(a) $\beta = 180°$

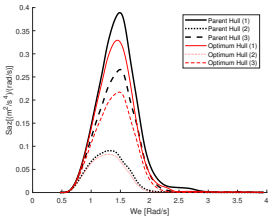

(b) $\beta = 120°$

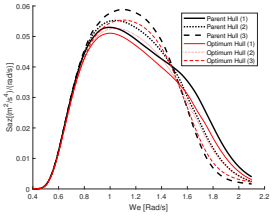

(c) $\beta = 90°$

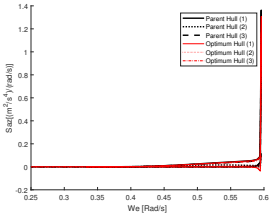

(d) $\beta = 60°$

Figure 13: Absolute vertical acceleration. Parent hull: SHIP1 ($C_B = 0.71$, LCB = 52%) Optimum hull: Set2 ($C_B = 0.76$, LCB = 50%) , at points 1, 2 and 3.

0.76, LCB = 50% obtained from Set 2. By comparing the vertical accelerations it is confirmed that the optimized hull based on OMSI also reduced its absolute vertical accelerations. However it is worth noticing that not all locations see its vertical accelerations being reduced, as shown in Figures 14(b) and 14(c). In such headings the hull transformations seem to be less desirable, noticing that by using a parameter such as OMSI, the overall results are being improved instead of only some particular conditions.

Table 25: Remote location points on SHIP1.

Description	Units	1	2	3	4	5	6
Longitudinal Position (+ fwd MS)	m	29	0	-35	29	0	-35
Offset from center line	m	0	0	0	-5	-5	-5

Table 26: Remote location points on SHIP2.

Description	Units	1	2	3
Longitudinal Position (+ fwd MS)	m	-36	-36	-36
Offset from center line	m	-6	0	6

5.4. Resistance analysis

The main focus of the present work has been on improving the seakeeping performance of passengers ships for comfort purposes. However such transformations my influence other performance parameter of a ship, as is the case of hull resistance. Therefore the hull resistance was assessed for each Set n of hull transformations. In this study it was concluded that the reductions in OMSI are generally associated with an increase in ship resistance. Only hull transformations using Set 5, increasing length at waterline L_{WL} are associated with both reductions on OMSI and hull resistance. It is then

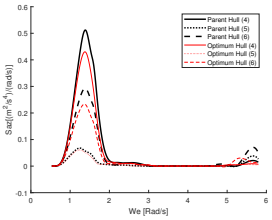

(a) $\beta = 180°$

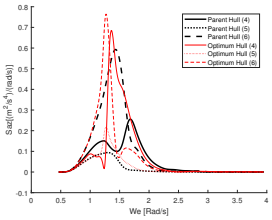

(b) $\beta = 120°$

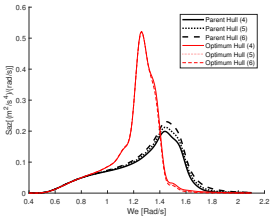

(c) $\beta = 90°$

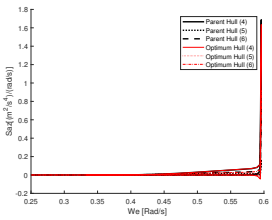

(d) $\beta = 60°$

Figure 14: Absolute vertical acceleration. Parent hull: SHIP1 ($C_B = 0.71$, LCB = 52%) Optimum hull: Set2 ($C_B = 0.76$, LCB = 50%) , at points 4, 5 and 6.

up to the naval architect to consider the priority of each parameter in a ships performance before performing any hull transformation.

5.5. Operability assessment of various hull variations with reduced OMSI

The operability index is a ratio, between the number of sea-sates (for all available peak periods) with significant wave heights, that do not exceed the maximum significant wave height (based on the seakeeping criteria), over the total number of sates (N) in a certain wave scatter diagram.

Two different criteria are selected namely, vertical accelerations and MSI. The criteria for vertical accelerations is that the maximum vertical acceler-

ation during an exposure of 2 hours at any point should be smaller than **0.05*g** (g being the gravitational acceleration). While for MSI is that the maximum MSI during an exposure of 2 hours at any point should be less than **35%**. Both criteria are based on Tezdogan et al. [19]. From the operability analysis it was confirmed that the optimized hulls based on the OMSI analysis are associated with an increase of ship operability based on the same comfort criteria that were minimized. It was also concluded that using a operability index that is based on pass/fail that discards any progress out of the criteria range is a less efficient approach compared to using a parameter like OMSI.

6. Conclusions

Two different passenger ships were used to study the comfort of passenger on the deck. The first ship (SHIP1) was set to operate on calm waters near the coast of Algarve (Operating Scenario 1) had multiple points of interest along the deck. The second ship (SHIP2) was set to operate on the Atlantic Ocean (Operating Scenario 2), connecting Algarve to Madeira and it only had a single area of interest. Six different sets of hull transformations were performed using *MAXSURF* Modeler [3]. For every new hull the parameter OMSI, was calculated using *MATLAB*, based on the results from *CENTEC-SK*. OMSI was used to compare the differences in passenger's comfort on each new hull transformation. Based on this analysis the following steps may be take to obtain an optimized hull for passenger's comfort:

- Increase block coefficient (C_B) by reducing draft (T) for a fixed midship coefficient (C_M), displacement, breath and waterline length.
- Shift the longitudinal center of buoyancy (LCB), depending on locations of interest, equilibrium and trim considerations.
- Decrease midship coefficient (C_M), while increasing prismatic coefficient (C_P) and waterplane coefficient (C_{WP}.)
- Increase waterline length (L_{WL}) for fixed B_{WL}/T ratio, displacement and form coefficients.
- Increase B_{WL}/T ratio for fixed waterline length (L_{WL}), displacement and form coefficients.

References

[1] F. Belga. *Seakeeping optimization of a fast displacement catamaran on the basis of strip-theory codes.* Tcnico Lisboa, 2017.

[2] F. Belga, M. Ventura, and C. G. Soares. Seakeeping optimization of a catamaran to operate as fast crew supplier at the alentejo basin. *C. Guedes Soares and T. A. Santos(Eds). Progress in Maritime Engineering and Technology, London, UK:Taylor & Francis*, 2018.

[3] I. Bentley Systems. *Maxsurf Modeler, Windows Version 21, User Manual.* Bentley Systems, Incorporated, 2017.

[4] I. Bentley Systems. *Maxsurf Motions, Windows Version 21, User Manual.* Bentley Systems, Incorporated, 2017.

[5] T. Cepowski. Influence analysis of changes of design parameters of passenger-car ferries on their selected sea-keeping qualities. *POLISH MARITIME RESEARCH 1(64) Vol 17; pp. 25-32*, 2010.

[6] J. L. Colwell. Human factors in the naval environment: a review of motion sickness and biodynamic problems. *Technical Report DREA-TM-89-220, Defence Research Establishment Atlantic, Dartmouth, Nova Scotio, Canada*, 1989.

[7] N. Fonseca and C. G. Soares. Time domain analysis of vertical ship motions. *Transaction on the Built Environment vol 5, WIT Press, ISSN 1743-3509*, 1994.

[8] G. J. Grigoropoulos and T. A. Loukakis. A new method for developing hull forms with superior seakeeping qualities. *Department of Na val Architecture and Marine Engineering, National Technical University of Athens, 42 October 28th, Athens, Greece*, 1988.

[9] ITTC. Summary of results obtained with computer programs to predict ship motions in six degree of freedom and related responses: comparative study on ship motion program. *15th & 16th ITTC seakeeping committee, Japan*, 1983.

[10] J. Journe and W. Massie. *OFFSHORE HYDROMECHANICS,First Edition.* Delft University of Technology, January 2011.

[11] A. Kukner and K. Sariöz. High speed hull form optimization for seakeeping. *Advances in Engineering Software, 22(3):179-189*, 1995.

[12] H. Lackenby. On systematic geometrical variation of ship forms. *RINA Transactions, Vol.92*, 1950.

[13] M. E. McCauley, J. W. Royal, C. D. Wylie, J. F. O'Hanlon, and R. R. Mackie. Motion sickness incidence: Exploratory studies of habituation, pitch and roll, and the refinement of a mathematical model. *Technical Report 1733-2, Human Factors Research Inc., Goleta, California*, 1976.

[14] J. F. O'Hanlon and M. E. McCauley. Motion sickness incidence as a funtion of the frequancy and acceleration of vertical sinusoidal motion. *Aerospace Medicine, vol.45(4), pp. 366-369*, 1974.

[15] S. Özüm, B. Sener, and H. Yilmaz. A parametric study on seakeeping assessment of fast ships in conceptual design stage. *Ocean Engineering 38 14391447*, 2011.

[16] J. Ramos and C. G. Soares. On the assessment of hydrodynamic coefficients of cylinders in heaving. *Ocean Engineering, 24(8):743-763*, 1997.

[17] N. Salvesen, E. O. Tuck, and O. Faltinsen. Ship motions and sea loads. *In Transactions of the Society of Naval Architects and Marine Engineers, SNAME, vol. 78, pp. 250-287*, 1970.

[18] A. Scamardella and V. Piscopo. Passenger ship seakeeping optimization by the overall motion sickness incidence. *Ocean Engineering 76 (2014) 86-97*, 2013.

[19] T. Tezdogan, A. Incecik, and O. Turan. Operability assessment of high speed passenger ships based on human comfort criteria. *Department of Naval Architecture, Ocean and Marine Engineering, University of Strathclyde, 100 Montrose Street, Glasgow, G4 0LZ, UK*, -.